



HAL
open science

Determination of object resonances by vibro-acoustography and their associated modes

Farid G. Mitri, Zine El Abiddine E.A. Fellah, Etienne Closset, Philippe
Trompette, Jean-Yves Chapelon

► **To cite this version:**

Farid G. Mitri, Zine El Abiddine E.A. Fellah, Etienne Closset, Philippe Trompette, Jean-Yves Chapelon. Determination of object resonances by vibro-acoustography and their associated modes. Ultrasonics, 2004, 42, pp.537-543. 10.1016/j.ultras.2004.01.050 . hal-00105759

HAL Id: hal-00105759

<https://hal.science/hal-00105759>

Submitted on 20 Jun 2022

HAL is a multi-disciplinary open access archive for the deposit and dissemination of scientific research documents, whether they are published or not. The documents may come from teaching and research institutions in France or abroad, or from public or private research centers.

L'archive ouverte pluridisciplinaire **HAL**, est destinée au dépôt et à la diffusion de documents scientifiques de niveau recherche, publiés ou non, émanant des établissements d'enseignement et de recherche français ou étrangers, des laboratoires publics ou privés.



Distributed under a Creative Commons Attribution - NonCommercial 4.0 International License

Determination of object resonances by vibro-acoustography and their associated modes

F.G. Mitri ^{*}, Z.E.A. Fellah, E. Closset, P. Trompette, J.Y. Chapelon

National Institute of Health and Medical Research, INSERM Unit 556, Therapeutic Ultrasound Research Laboratory, 151 Cours Albert Thomas, 69424 Lyon Cedex 03, France

Vibro-acoustography technique known by its noncontact excitation was used to detect resonance frequencies of objects in water. Two intersecting ultrasound beams generated by a 40 mm-diameter annular array transducer, focused at 35 mm and driven at $f_1 = 2.2$ MHz and $f_2 = 2.22$ MHz respectively, were targeted inside the object under test to produce a radiation force beating at the difference frequency $f_2 - f_1$. This low frequency radiation force was used to excite the resonance vibration modes of the object by sweeping the frequency f_2 between 2.22 and 2.275 MHz. The amplitude of the acoustic emission produced by the vibrations of the object was detected by a low frequency hydrophone (BW = 60 kHz). By this approach, it was possible to detect resonance frequencies through amplitude variations of the measured acoustic emission. Experiments were conducted in a water tank for objects of different shapes and sizes. With a chalk sphere (15 mm-diameter) two resonance frequencies were detected at 45.75 and 68.75 kHz, and with a cylinder (10.38 mm-diameter and 32.20 mm-length) four principal resonance frequencies were identified in the 60 kHz-bandwidth of the hydrophone. It was shown with finite element calculations performed with Ansys, in which both solid and fluid parts were modelled, that the measured resonance frequencies corresponded to compressional or dilatation vibration modes of the object. It was verified that shear waves generated by torsional vibration modes were not propagated in water, as it is well known. The use of this technique to characterize heterogeneities in different media seems to be relatively more advantageous to other ultrasonic methods.

Keywords: Vibro-acoustography; Resonance frequency; Radiation force; Finite-element simulations

1. Introduction

The study of objects in terms of their mechanical response to external forces is of considerable interest in a variety of scientific fields. The fatigue or cracks of a material modify the mechanical properties. Similarly, soft tissues can be characterized from their elastic properties that often change in presence of pathology. In resonant ultrasound spectroscopy (RUS) [1], a sample with known size and mass is joined between an ultrasound source and a detector to measure its resonance frequencies. The resonances are related to mechanical parameters, including the elastic constants of the material. In some cases, it is required to use a noncontact

excitation especially for biomedical applications in order to characterize heterogeneities. Vibro-acoustography [2] is a noncontact method that uses a highly localized low frequency stimulation radiation force to remotely excite the object and measures its frequency response by means of a hydrophone. It allows to avoid physical contact with the object under test in both the excitation and detection procedures. This method is capable of exerting an oscillatory force in a confined region of the object, and the frequency response can be measured in a wide frequency range. These features make vibro-acoustography a potential tool for material characterization. In this work, we use vibro-acoustography in exploring a wide frequency range, to detect resonance frequencies of chalk sphere and cylinder samples. A systematic comparison with numerical calculations is also proposed. Results show that the acoustic emission is maximal at the object's resonance frequencies that are related to

^{*} Corresponding author. Tel.: +33-47268-1930/36; fax: +33-47268-1931.

E-mail address: mitri@ieee.org (F.G. Mitri).

dilatation and bending vibrational modes. Thus, it can be stated that by being positioned at any a priori resonance frequency of the object under test, the frequency response is optimal easing its detection, even if its dimensions are small.

2. Method and materials

2.1. Vibro-acoustography method

Vibro-acoustography uses radiation force of amplitude modulated focused ultrasound to vibrate the object at an arbitrary low frequency. Object vibration produces a sound field in the medium named acoustic emission which is function of its mechanical properties. By measuring the resulting variations of the emission field, one can estimate some of its mechanical parameters.

Fig. 1 shows a vibro-acoustography system. A two-element confocal ultrasound transducer is focused inside the object. Each of the two elements is driven by a burst source at frequencies equal to f_1 and $f_2 = f_1 + \Delta f$, respectively. The beams interact only in a small region, i.e. the focal spot. The change of energy density due to the discontinuity of impedance produces a radiation force component in the beam direction [3]. This force is oscillatory in response to the temporal variations in the energy density caused by the amplitude modulation, hence, it vibrates the object at Δf . If the excitation force frequency corresponds to a natural mode, resonance will occur, which will produce compressional and shear wave motions inside the object. Object vibration elicits a sound field in the medium which is detected by a nearby hydrophone and recorded after digitization. The amplitude of the acoustic emission signal is [4]:

$$\Phi(\Delta f) = Cd_r H(\Delta f) Q(\Delta f) \quad (1)$$

where C is a constant proportional to the intensity of the primary ultrasound beams, $Q(\Delta f)$ is a complex function representing the mechanical frequency response or admittance of the object at the selected point, and $H(\Delta f)$ represents the transfer function of the propagation medium and receiver, which is assumed to be fixed and known. The resonance frequency(ies) of the object can be determined by varying Δf within the range of interest while keeping the amplitude of the primary ultrasound beams constant, and recording the resultant acoustic emission $\Phi(\Delta f)$ from the object. $\Phi(\Delta f)$ depends directly on the product of both the drag coefficient d_r and the mechanical admittance $Q(\Delta f)$ of the object. In general, the drag coefficient shows maxima and minima [5,6] related to certain resonances for wide variations in frequency. However in our case, the drag coefficient is directly dependent on f_1 and f_2 , and is of constant amplitude while sweeping f_2 between 2.220 and 2.275 MHz (low frequency variations (20–75 kHz bandwidth)). Acoustic emission variations (peaks of $\Phi(\Delta f)$) are therefore determined only from the resonances of $Q(\Delta f)$. In water and for low amplitudes, ultrasound absorption is very weak to cause streaming that is also another nonlinear phenomenon inducing object's excitation. Consequently, its effect is neglected in this work.

2.2. Equipment

Spherically focused piezoelectric transducer divided into two equal area elements produces the two focused ultrasound fields. The annular transducer has a diameter of 40 mm with a focal distance of 35 mm and a natural resonance frequency of 2.20 MHz. Driving signals for

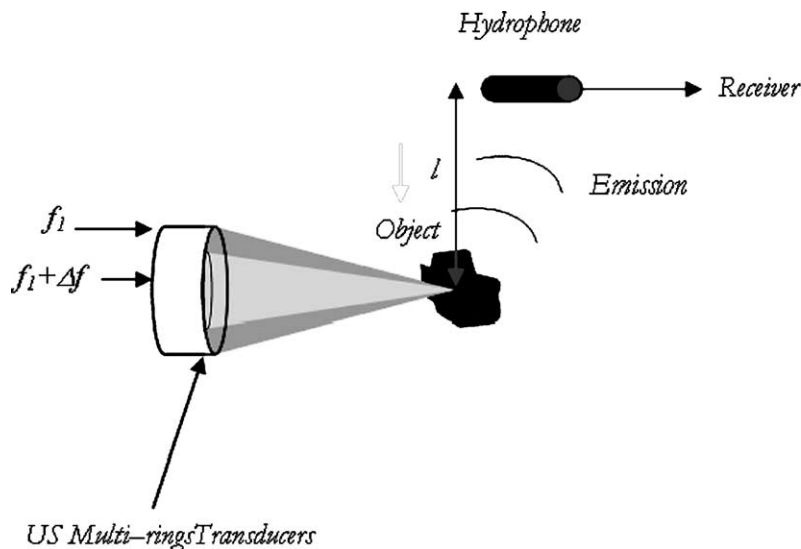


Fig. 1. Vibro-acoustic system.

the elements were obtained from two RF-amplifiers (KMP Electronics) that were modulated by two function generators (HM 8131-2 Hameg) both controlled by a pulse generator (8112 A HP). The transducer was mounted on a 3-D positioning system (Micro-contrôle) and immersed in a tank of degassed water. The low frequency signal was registered using a hydrophone (SQ 03 Sensor) preamplified, band-pass filtered (AF 420 Multimetrics) in the 10–80 kHz range and recorded by digital oscilloscope (2340 A Tektronix). The data was then transferred via an IEEE-488 communication BUS to a PC controlling the positioning system.

2.3. Experiments

The experimental setup is shown in Fig. 1. The first object is a chalk sphere (15 mm-diameter) placed at the focal plane of the ultrasound beams in the water tank. The mechanical properties are Young’s modulus, $E_0 = 4.1$ GPa, Poisson’s ratio, $\nu = 0.26$ [7] and mass density $\rho = 1086$ kg/m³. It is well established that water affects the mechanical properties of the porous chalk material. The sphere porosity is estimated as the ratio M_0/M where M_0 is the measured mass in air and M is the ‘wetted mass’ measured after soaking the sphere in water for 1 h. Porosity is equal 25%. The effective Young’s modulus is calculated using the Duckworth–Knudsen equation [8]:

$$E = E_0 \exp(-bP) \quad (2)$$

where E is Young’s modulus, E_0 is Young’s modulus at zero porosity, P is porosity and b is a variable porosity correction factor, set at unity. Consequently, the effective Young’s modulus of the sphere, taking porosity into account, is $E = 3.19$ GPa, which will be used in the numerical simulations.

The second object under test is a blackboard chalk cylinder (10.38 mm-diameter and 32.20 mm-length). Its mass density is $\rho = 1314$ kg/m³. The Young’s modulus of the chalk is determined experimentally using a vibration test and was found to be $E_0 = 3.02$ GPa. The cylinder’s porosity was 31%. The effective Young’s modulus, according to Eq. (2) was then $E = 2.215$ GPa. The cylinder suspended horizontally with the ultrasound beams perpendicular to its axis, was placed at the transducer’s focus.

2.4. Finite-element simulations

A coupled harmonic acoustic analysis was performed on Ansys [9] to predict the pressure distribution in the fluid in the case of an harmonically varying load. The driving nodal forces on both the sphere and cylinder were applied at their centers. In the finite element harmonic analysis, a step frequency of 0.5 kHz was used. It was verified that the response does not vary significantly when the step value is decreased. The amplitude of the driving force is assumed to be of constant value while sweeping frequency. The coupled acoustic analysis involves modelling the fluid medium surrounding the

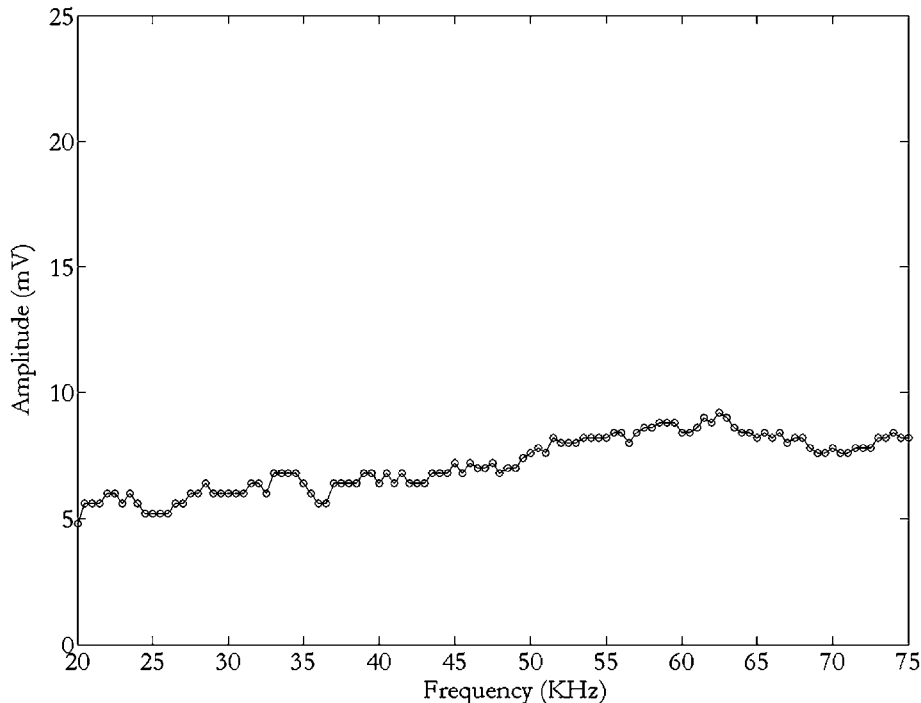


Fig. 2. Low frequency signal amplitude in water.

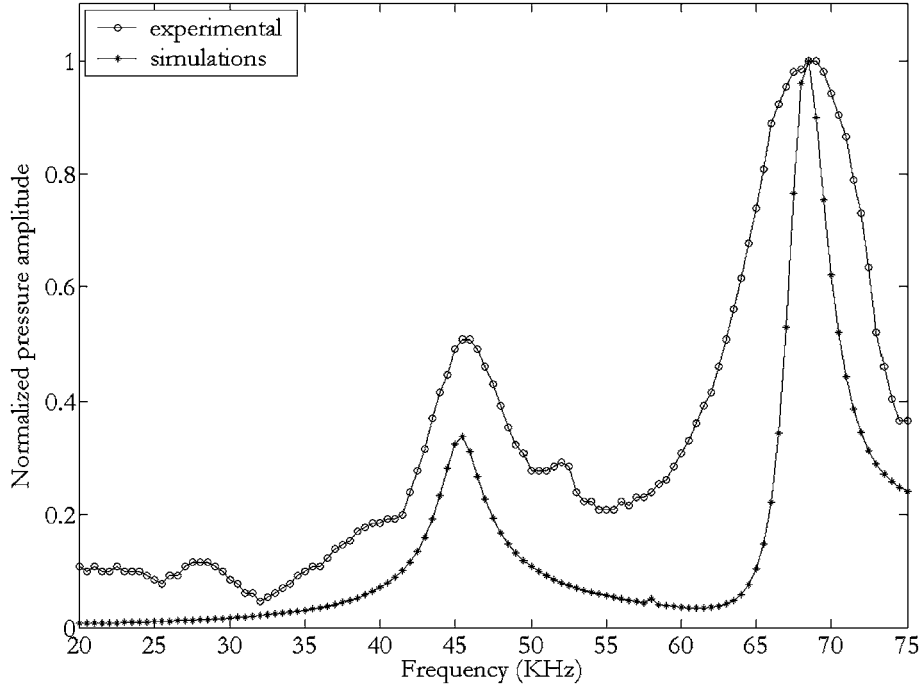


Fig. 3. Experimental and simulated vibro-acoustic amplitude response from the chalk sphere.

structure, taking the fluid–structure interaction into account. The pressure amplitude has been calculated in the fluid. The pressure distribution was determined in the 20–75 kHz frequency range. One particular node in the fluid was chosen and it was verified that the responses at neighbouring nodes are comparatively the same.

The fluid medium was modelled by 3-D linear fluid elements surrounding the solid, and 2-D linear absorbing elements at the external boundary simulating the outgoing propagation effects of a domain extending to infinity. Absorbing elements eliminate reflections and therefore interference with vibration of the solid structure.

The chalk sphere was modelled using 3-D tetrahedral linear solid elements. The total numbers of nodes and elements was 2488 and 12,629, respectively.

The chalk cylinder was also modelled using the same elements as were used for the sphere, and the total numbers of nodes and elements was 1081 and 4829, respectively.

After performing the harmonic analysis, a modal analysis was achieved in the fluid medium in order to identify the vibrational mode associated with its correspondent resonance frequency.

3. Results

Fig. 2 shows the low frequency signal amplitude in the water tank without an object. This was measured to verify that the water tank’s resonance frequencies are

Table 1

Comparison of resonance frequencies for a chalk sphere calculated experimentally, and by simulations

Sphere	Resonance frequencies values (kHz)	
Experimental	45.75	68.75
Simulations (harmonic analysis)	45.5	68.5

outside the chosen bandwidth, so there was no interference with the structure’s vibrations.

Fig. 3 shows the combined experimental and simulated frequency response of the sphere (acoustic emission amplitude versus frequency). Two main resonance frequencies are observed in the 20–75 kHz frequency range (Table 1).

Fig. 4 shows the combined experimental and simulated frequency response of the cylinder (acoustic emission amplitude versus frequency). Four main resonance frequencies are detected in the 20–75 kHz frequency range (Table 2).

4. Discussion

In this paper, the frequency response of immersed objects was detected using a noncontact excitation method. Two and four experimental resonance frequencies are clearly detected for the sphere and cylinder, respectively. Both numerical harmonic and modal analyses using the finite element method were

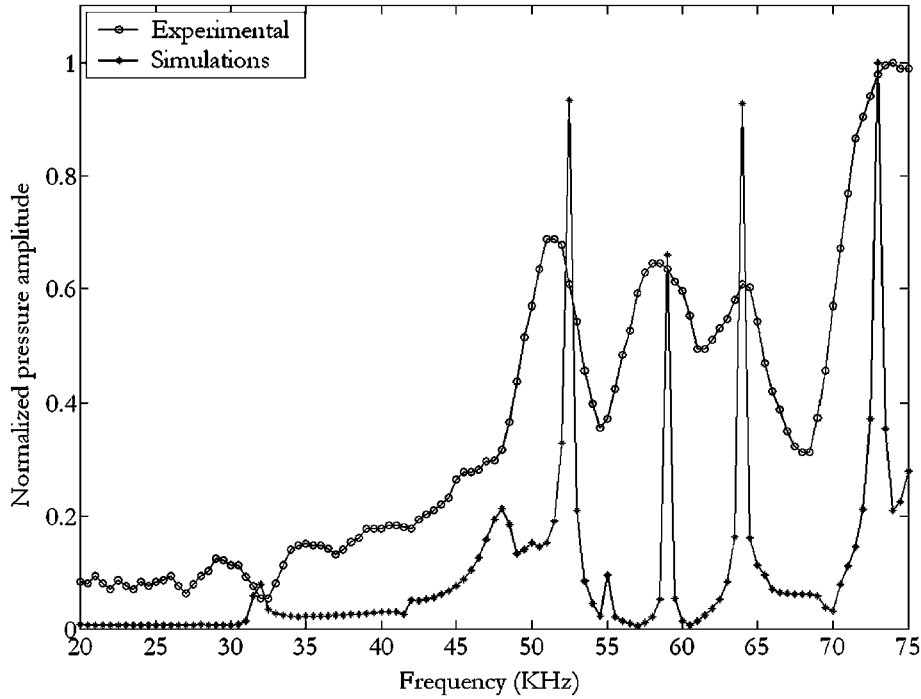


Fig. 4. Experimental and simulated vibro-acoustic amplitude response from the chalk cylinder.

Table 2
Comparison of resonance frequencies for a chalk cylinder calculated experimentally and by simulations

Cylinder	Resonance frequencies values (kHz)			
Experimental	51.25	58.25	64	74
Simulations (harmonic analysis)	52.5	59	64	73

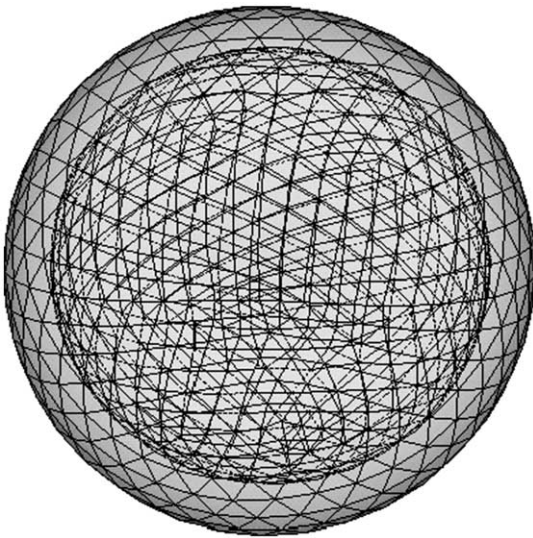


Fig. 5. Sphere's dilatation mode at 45.5 kHz (undeformed and deformed shapes).

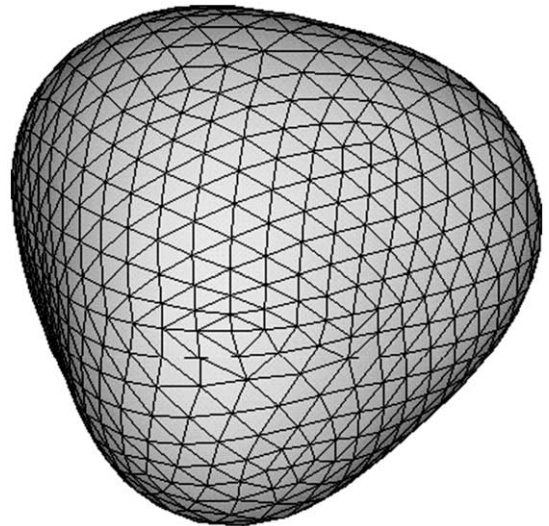


Fig. 6. Sphere's dilatation mode at 68.5 kHz.

performed in order to give an interpretation of the experimental results. The harmonic numerical results show very good agreement with the experiments (Figs. 3 and 4). A coupled acoustic modal analysis, taking the fluid-structure interaction into account, was performed to visualize each mode Φ_i associated with the corresponding resonance frequency f_i for both models.

For the spherical model, the modal analysis printed out several types of mode shapes. The two main

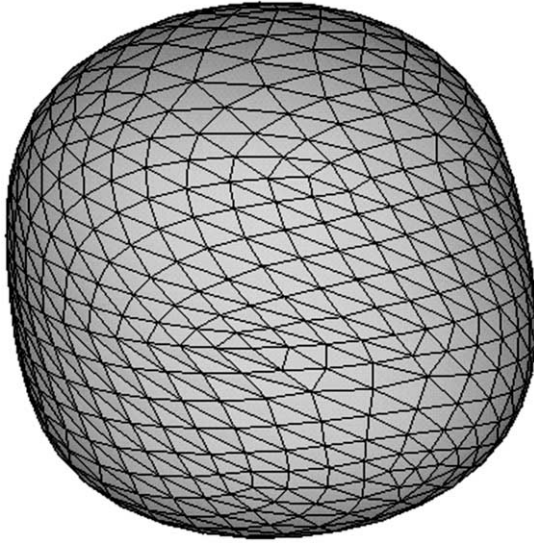


Fig. 7. Sphere's torsional mode.

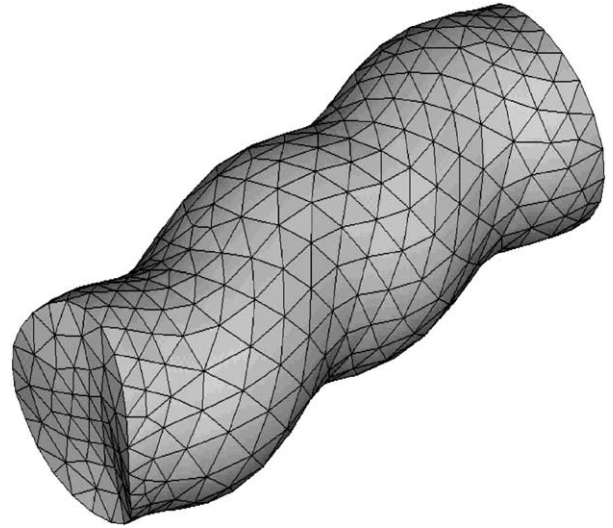


Fig. 9. Cylinder's bending mode.

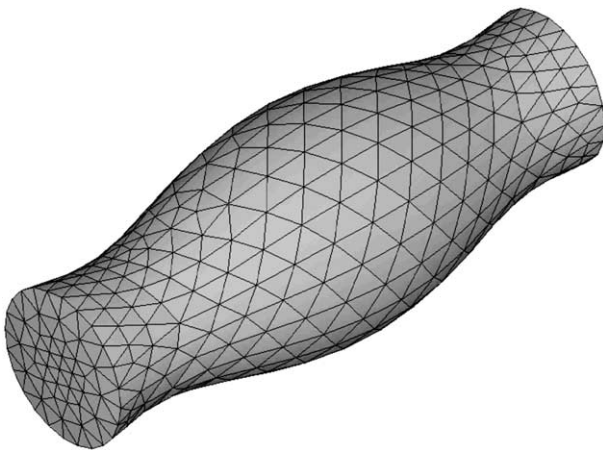


Fig. 8. Cylinder's breathing mode.

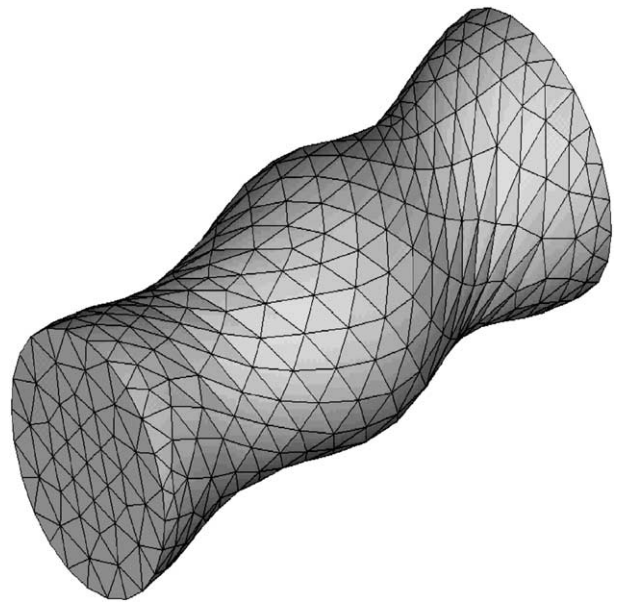


Fig. 10. Cylinder's torsional mode.

resonance frequencies detected at 45.5 and 68.5 kHz, were identified to dilatation modes (Figs. 5 and 6), respectively. A third normal mode was detected by modal analysis at 58 kHz. It was found to be a torsional vibration mode (Fig. 7) generating shear waves that are not propagated in the fluid medium and consequently are not detected by the hydrophone.

As for the cylinder model several types of mode shapes were computed from the modal analysis. The main resonance frequency at 50.5 kHz was identified to a breathing vibrational mode (Fig. 8) and the three others to bending vibrational modes (Fig. 9). A complex vibrational shear mode was detected at 29.8 kHz by the modal analysis (Fig. 10) that was not identified experimentally. The main cause is also that this mode generates torsional waves that are not propagated in water.

Hence, it was concluded that only compression waves resulting from dilatation, breathing and bending modes are propagated in the fluid medium, as it is well known.

The sharpness of the experimental peaks differs from that predicted by the simulations. The main reason is that damping plays an important part, since an arbitrary value for the chalk material is used in the Ansys simulations ($\xi = 0.005$), while the experimental measurements presented are naturally damped by inter-granular friction.

Results for the sphere correlated particularly well with the simulations because spherical geometry provides isotropic acoustic emission.

Because of the flat response of the water tank without object, the propagation medium has no significant effect on determination of the object's resonance frequencies (Fig. 2).

The temperature was fixed during the experiments; therefore its influence on the acoustic emission signal and the resonance frequencies was ignored.

The model developed and presented here gives good quantitative results for the detection of resonance frequencies. An assumption in this model is that the fluid medium surrounding the sphere and cylinder is homogeneous. An experimental verification of this method is currently under investigation, in order to detect heterogeneities in soft tissues, such as kidney stones during lithotripsy treatment and radioactive metal seeds in brachytherapy sessions.

5. Conclusion

Vibro-acoustography shows once more its capability of measuring accurately the of immersed objects' resonance frequencies. A finite element model using harmonic and modal analyses is developed to investigate the frequency response of materials. The simulations correlate well with experimental results. It has been concluded that some resonance frequencies can be de-

tected and are related to dilatation and bending vibrational modes. Additional work must focus on using these detectable resonances improving performances of vibro-acoustography in biomedical applications, such as characterization of heterogeneities in tissue.

Acknowledgements

This work was supported by Grant No. 01-2-93-0314 of an RNTS project from the French Ministry of Economy, Finance and Industry.

References

- [1] J. Maynard, *Phys. Today* 49 (1996) 26.
- [2] M. Fatemi, J.F. Greenleaf, *Science* 280 (1998) 82.
- [3] P.J. Westervelt, *J. Acoust. Soc. Am.* 23 (1951) 312.
- [4] M. Fatemi, J.F. Greenleaf, *Ultrason. Imaging* 21 (1999) 141.
- [5] L.W. Anson, R.C. Chivers, *J. Acoust. Soc. Am.* 69 (1981) 1618.
- [6] T. Hasegawa, K. Yosioka, *J. Acoust. Soc. Am.* 46 (1969) 1139.
- [7] D. Heimbach, R. Munver, P. Zhong, J. Jacobs, A. Hesse, S.C. Müller, G.M. Preminger, *J. Urol.* 164 (2000) 537.
- [8] R.W. Rice, in: R.K. MacCrone (Ed.), *Treatise on Materials Science and Technology*, vol. 11, Academic Press, New York, 1977, p. 200.
- [9] Ansys Inc. Software.